N. Jb. Miner. Abh. **179** 3 265–294 Stuttgart, Januar 2004

Two new minerals, rondorfite, $Ca_8Mg[SiO_4]_4Cl_2$, and almarudite, $K(\square,Na)_2(Mn,Fe,Mg)_2(Be,Al)_3[Si_{12}O_{30}]$, and a study of iron-rich wadalite, $Ca_{12}[(Al_8Si_4Fe_2)O_{32}]Cl_6$, from the Bellerberg (Bellberg) volcano, Eifel, Germany

Tamara Mihajlović, Christian L. Lengauer, Theodoros Ntaflos, Uwe Kolitsch and **Ekkehart Tillmanns,** Wien

With 5 figures and 14 tables

MIHAJLOVIĆ, T., LENGAUER, C. L., NTAFLOS, T., KOLITSCH, U. & TILLMANNS, E. (2004): Two new minerals, rondorfite, $Ca_8Mg[SiO_4]_4Cl_2$, and almarudite, $K(\square,Na)_2(Mn,Fe,Mg)_2(Be,Al)_3[Si_{12}O_{30}]$, and a study of iron-rich wadalite, $Ca_{12}[(Al_8Si_4Fe_2)O_{32}]Cl_6$, from the Bellerberg (Bellberg) volcano, Eifel, Germany. – N. Jb. Miner. Abh. **(179):** 265–294; Stuttgart.

Abstract: Rondorfite, almarudite and iron-rich wadalite have been found in xenoliths in leucite–tephrite lava from a quarry at the Bellerberg (Bellberg) volcano lava field (near Ettringen), 2 km north of Mayen, Eastern Eifel volcanic area, Germany. Rondorfite, not uncommon in Ca-rich xenoliths at this locality, forms anhedral grains (<0.3 mm) intergrown with ternesite. Both are embedded in a carbonate–quartz matrix and are associated with ettringite/thaumasite, mayenite, cuspidine, larnite, "calcio–olivine", tobermorite, portlandite, hydrocalumite, a member of the ellestadite series, magnetite and hematite. Rondorfite is orange brown to amber, with a light amber streak and vitreous lustre. It is brittle, with no cleavage, has conchoidal fracture and D_{calc} is 3.034 g/cm^3. Optically, it is isotropic, with n = 1.676(1). Electron microprobe analysis yielded (wt.%): Na_2O 0.07, MgO 4.52, CaO 57.05, FeO 0.54, Al_2O_3 0.40, SiO_2 30.51, TiO_2 0.13, Cl 6.71 ($-O \equiv Cl$), sum 99.93, giving the empirical formula $(Ca_{7.98}Na_{0.02})(Mg_{0.87}Fe_{0.06}Al_{0.06})^{[4]}[(Si_{3.98}Ti_{0.01})O_{16}](Cl_{1.92}OH_{0.08})$, based on O = 16+1. Rondorfite is cubic, space group $Fd\bar{3}$ (no. 203), contrasting with $Fd\bar{3}m$ (no. 227) reported for a synthetic crystal. It has a = 15.0850(3) Å, V = 3432.7(1) Å^3 and Z = 8. Strongest lines in the X-ray powder diffraction pattern are: 2.666 (100) *440*, 1.540 (50) *844*, 2.901 (40) *511*, 1.964 (16) *553*, 2.549 (30) *531*, 1.885 (30) *800* [*d* in Å (I) *hkl*]. A single-crystal structure refinement ($R1$ = 2.31 %) showed that the structure consists of four isolated SiO_4 tetrahedra linked via a central MgO_4 tetrahedron, thus forming a $[MgSi_4O_{16}]^{-14}$ pentamer. These pentamers are connected through O–Ca–O bonds.

DOI: 10.1127/0077-7757/2004/0179-0265 0077-7757/04/0179-0265 $ 7.50

Almarudite has been found in a single silicate-rich xenolith. It forms euhedral, platy crystals flattened on {0001}, with a maximum diameter of about 1.5 mm and a maximum tickness of 0.2 mm. It is associated with tridymite, sanidine, "clinopyroxene", "amphibole", quartz, hematite, sillimanite and rare braunite. Almarudite is yellow to orange, with light orange streak and vitreous lustre. It is brittle with irregular fracture and no cleavage, and D_{calc} is 2.714 g/cm^3. Optically, almarudite is uniaxial negative, with n_ω = 1.560(1) and n_ε = 1.559(1) and a strong pleochroism from orange ($//n_\omega$) to colourless ($//n_\varepsilon$). Electron microprobe analyses yielded (wt.%): Na_2O 0.66, K_2O 4.05, BeO 5.18, MgO 1.51, CaO 0.12, MnO 7.31, FeO 4.48, ZnO 0.24, Al_2O_3 4.09, SiO_2 72.31, sum 99.95 (BeO determined by LAM–ICP–MS), giving the empirical formula $K_{0.86}{}^{[12]}Na_{0.21}{}^{[9]}(Mn_{1.03}Fe_{0.62}Mg_{0.37}Zn_{0.03}Ca_{0.02})^{[6]}(Be_{2.09}Al_{0.79})^{[4]}[Si_{12}O_{30}]$, based on Si = 12. Almarudite is hexagonal, space group *P6/mcc* (no. 192), with a = 9.997(1), c = 14.090(1) Å, V = 1219.5(2) Å^3, and Z = 2. Strongest lines in the X-ray powder diffraction pattern are: 2.882 (100) *114*, 3.187 (90) *211*, 4.076 (80) *112*, 2.732 (50) *204*, 7.047 (40) *002*, 5.000 (40) *110* [*d* in Å (I) *hkl*]. A single-crystal structure refinement ($R1$ = 1.85 %) confirmed that the structure is isotypic to milarite and related $A^{[12]}B_2{}^{[9]}M_2{}^{[6]}T2_3{}^{[4]}[T1_{12}O_{30}]$ compounds. The *A* site is dominated by K, the *B* site is partially occupied by Na, and the *M* site is clearly dominated by Mn+Fe over Mg. The chemistry at the *T2* site can be refined to a Be/(Be+Al) value close to 0.75; the *T1* site is occupied by Si. Type material of rondorfite (M8874) and almarudite (N1190) have been deposited at the mineral collection of the Naturhistorisches Museum Wien (NHMW), Austria.

The Fe-rich wadalite, found in a Ca-rich xenolith from the Bellerberg, is characterised by electron microprobe analyses and X-ray methods. Optically, the lemon-yellow, tristetrahedral crystals are isotropic, with n = 1.700(1), D_{calc} = 3.105 g/cm^3. Electron microprobe analysis yielded (wt.%): MgO 1.68, CaO 41.55, Al_2O_3 23.06, Fe_2O_3 8.06, SiO_2 15.66, TiO_2 0.72, Cl 9.79 ($-O \equiv Cl$), sum 100.52, giving the empirical formula $Ca_{12.00}[(Al_{7.10}Si_{4.54}Fe_{1.34}Mg_{0.87}Ti_{0.15})O_{31.99}]Cl_{5.84}$ assuming a sum of cations of 26. In the rim of the crystals, the coupled substitution $Mg^{2+}+Si^{4+} \leftrightarrow Al^{3+}+Fe^{3+}$ is observed. The cubic mineral crystallises in space group $I\bar{4}3d$ (no. 220), with a = 12.0343(2) Å, V = 1742.9(1) Å^3 and Z = 2. Strongest lines in the X-ray powder diffraction pattern are: 2.691 (100) *420*, 3.008 (48) *400*, 2.456 (46) *422*, 1.669 (34) *640*, 1.608 (31) *642*, 2.360 (21) *510* [*d* in Å (I) *hkl*]. The structure refinement ($R1$ = 2.38 %) confirms isotypy with the mayenite group compounds, $M_{12}[T2_8T1_6O_{32}]X$ ($X = O^{2-}$, S^{2-}, $2F^-$, $2OH^-$, $2Cl^-$), which can be classified as a 3,4-connected, interrupted framework structure. Based on the single-crystal structure refinement and bond-valence calculations the structural formula can be calculated as $Ca_{12.00}[(Si_{3.88}Al_{2.65}Fe_{1.32}Ti_{0.15})(Al_{4.73}Mg_{0.68}Si_{0.30}Fe_{0.29})O_{32}]Cl_{5.69}$.

Key words: rondorfite, almarudite, wadalite, new mineral, Bellerberg, Eifel area, milarite group, osumilite group, mayenite group, penta–aluminosilicates, interrupted framework.

Introduction

This article describes two new mineral species, rondorfite and almarudite, found in xenoliths from the Bellerberg volcano near Ettringen, located within the Quaternary volcano region around the Laacher See in the Eastern Eifel area, Germany. The Bellerberg (also named Bellberg or Bell-Berg) is a locality famous for unusual and new mineral species formed due to the interaction of silicate- or Ca-rich xenoliths with a leucite–tephrite lava (e.g. IRRAN et al. 1997, EFFENBERGER et al. 1998, KRAUSE et al. 1999). Geology, petrology and mineralogy were discussed and compiled by FRECHEN (1971), HENTSCHEL (1987) and SCHÜLLER (1990). In addition, the occurrence of an iron-rich wadalite, a rare mineral of the mayenite group, from the same locality is characterised using quantitative chemical analyses, optical data and a single-crystal structure refinement.

The synthetic analogue of rondorfite, ideally $Ca_8Mg[SiO_4]_4Cl_2$, has already been thoroughly characterised by YE & WANG (1985) and YE et al. (1987), who reported the synthesis of single crystals, the crystal structure (space group $Fd\bar{3}m$, $R = 7.3\,\%$; ICSD-entry 68–243), and several physical and chemical characteristics by means of IR-spectroscopy, thermal analyses, and X-ray powder diffractometry. These authors observed a decomposition temperature of about 1265 °C in air. Independently of YE et al. (1987), the synthesis, crystal structure and some properties of synthetic rondorfite were also reported by VON LAMPE et al. (1986) who, in contrast, reported space group $Fd\bar{3}$. More recent X-ray powder diffraction data of $Ca_8Mg[SiO_4]_4Cl_2$ are given in the ICDD database with entries 41–248 and 50–1546. Synthetic rondorfite has, in the last decade, attracted some interest as a host for luminescent REE cations: ZHANG & LIU (1992) discussed the luminescence properties of synthetic, Eu^{2+}-doped rondorfite powders. LIN et al. (2002) investigated the luminescence of synthetic, Ce^{3+}–Eu^{2+}-codoped rondorfite materials. The incorporation of Sr into synthetic, Eu^{2+}-doped rondorfite was studied by PARK et al. (1994). The first natural occurrence of $Ca_8Mg[SiO_4]_4Cl_2$ fits very well into the mineralogical and petrological environment of the Bellerberg parageneses of Ca-rich xenoliths, first investigated in detail by HENTSCHEL (1964) and JASMUND & HENTSCHEL (1964). Rondorfite is named in honour of ALICE and EUGEN RONDORF, two distinguished mineral collectors, who found this mineral together with BERND TERNES in 1979.

Almarudite is a new manganese-rich analogue of milarite, ideally $K(\square, H_2O)_2Ca_2(Be,Al)_3[Si_{12}O_{30}]$, which is also sometimes classified as a member of the osumilite group minerals. Up to now no synthetic analogue is known and it is the first finding of a beryllium-rich mineral in the volcanic rocks of the Eifel region. The occurrence, however, is in a good agreement with that of

the previously reported isotypic minerals eifelite, roedderite, osumilite and osumilite–Mg from the silicate-rich xenoliths of the Bellerberg (HENTSCHEL 1987). Almarudite was found by ALICE and EUGEN RONDORF in 1982. It is named in honour of the authors' hosting and supporting institution, the 'Universität Wien', and is derived from the university's proper name 'ALma MAter RUDolphina'.

Also in a Ca-rich xenoliths from the Bellerberg, which were collected by ALICE & EUGEN RONDORF in 1978 and BERND TERNES in 1990, the unusual occurrence of a Si- and Cl-containing 'mayenite' of lemon-yellow colour was observed. Further chemical and structural investigations revealed the mineral to be wadalite, ideally $Ca_{12}[(Al_{10}Si_4)O_{32}]Cl_6$, which was originally described from a skarn xenolith in a two-pyroxene andesite at Fukushima, Japan, by TSUKIMURA et al. (1993). They reported the crystal structure (space group $I\bar{4}3d$, $R = 6.2\,\%$; ICSD-entry 72–504) and noted that structural and other characteristics of the mineral are very similar to those of grossular. A comprehensive compilation on the structural relationships is given by GLASSER (1995). Wadalite has remained a very rare mineral, with less than about five localities reported at present.

Prior to publication, mineral species status and name of rondorfite (1997–013) and almarudite (2002–48) have been approved by the IMA Commission on New Minerals and Mineral Names and were briefly reported by LENGAUER et al. (1997) and MIHAJLOVIĆ et al. (2002), respectively. The investigated type materials are preserved at the mineral collection of the Naturhistorisches Museum Wien (NHMW), Austria, with catalog numbers M8874 (rondorfite) and N1190 (almarudite).

Occurrence and paragenesis

All three investigated minerals were found in an active quarry of the firm 'A. Caspar' at the Bellerberg (Bellberg) volcano lava field (near Ettringen) 2 km north of Mayen, in the Laacher See region, Eastern Eifel area, Germany. Rondorfite and the containing assemblage were formed during a metasomatic modification of limestone xenoliths enclosed in a Quaternary leucite–tephrite lava. In the samples studied, rondorfite occurs intergrown with the unnamed natural analogue of $Ca_2SiO_4 \cdot 0.5H_2O$, in association with ettringite/thaumasite, mayenite, ternesite, cuspidine, larnite, "calcio–olivine", tobermorite, portlandite, hydrocalumite, a member of the ellestadite series, and minor amounts of magnetite and hematite. The type material consists of anhedral grains intergrown with ternesite, both embedded in a carbonate–quartz matrix containing subordinate amounts of hematite and magnetite. In a similar paragenesis of another Ca-rich xenolith from the Bellerberg, euhedral crystals of

an iron-rich wadalite occur together with ettringite, gypsum, reinhardbraunsite, fluorite, cuspidine, a member of the ellestadite series, and gehlenite.

In contrast to rondorfite and wadalite, almarudite was formed during a pyrometamorphic modification of a silicate-rich xenolith enclosed in the leucite–tephrite lava. The type material consists of euhedral, platy crystals, which occur in cavities of the xenolith together with euhedral tridymite, sanidine, "clinopyroxene", "amphibole", quartz, hematite and rare braunite. Sillimanite occurs as rare fibrous masses in parts of the matrix of the xenolith. Beside the previously mentioned members of the milarite group also mullite, cordierite, powellite, bixbyite or rhönite are already known from such parageneses (HENTSCHEL 1987).

Physical and optical properties

Rondorfite grains are anhedral, <0.3 mm in diameter, and show orange brown to amber colour, vitreous lustre, and a light amber streak. Rondorfite is brittle and exhibits conchoidal fracture and no cleavage. It is isotropic, with n = 1.676(1) at λ = 589 nm and 24 °C; the density is calculated as 3.034 g/cm^3. The compatibility index according to the Gladstone-Dale relationship (MANDARINO 1981) is 0.0045, which is classified as excellent.

Almarudite forms euhedral thick tabular crystals flattened on {0001}, with a maximum diameter of about 1.5 mm and a thickness of up to 0.2 mm (Fig. 1). Beside the dominant hexagonal basis, additional forms are $\{10\bar{1}0\}$, $\{10\bar{1}2\}$ and $\{11\bar{2}0\}$. The ratio $a:c$ calculated from the cell parameters is 1.409. The colour varies from yellow to orange and the crystals show a glassy lustre and a light orange streak. Almarudite is brittle, with irregular fracture and no cleavage. For the optical examinations hand-picked almarudite fragments were mounted on glass fibres and inspected under a polarising microscope equipped with a spindle stage. It is uniaxial negative, with n_ω = 1.560(1), n_ε = 1.559(1) at λ = 589 nm and 24 °C; however, anomalous extinction, small biaxiality and zoning are common, as is also reported for osumilite from the Bellerberg (SCHREYER et al. 1983). Pleochroism is strong, from orange ($//n_\omega$) to colourless ($//n_\varepsilon$). The calculated density is 2.714 g/cm^3, and the compatibility index equals 0.0032, which is classified as excellent.

At the Bellerberg, the investigated iron-rich wadalite forms lemon-yellow, transparent crystals up to 0.5 mm in diameter (Fig. 2). An idealized crystal drawing is given by HENTSCHEL (1987). The dominant form is the tristetrahedron {211}, the corners of which are truncated by the negative $\{21\bar{1}\}$ form. It exhibits a vitreous lustre and a colourless streak. Optically, iron-rich wadalite is isotropic with n = 1.700(1) at λ = 589 nm and 24 °C. The density is calculated as 3.106 g/cm^3, and the compatibility index is 0.0088, which is classified

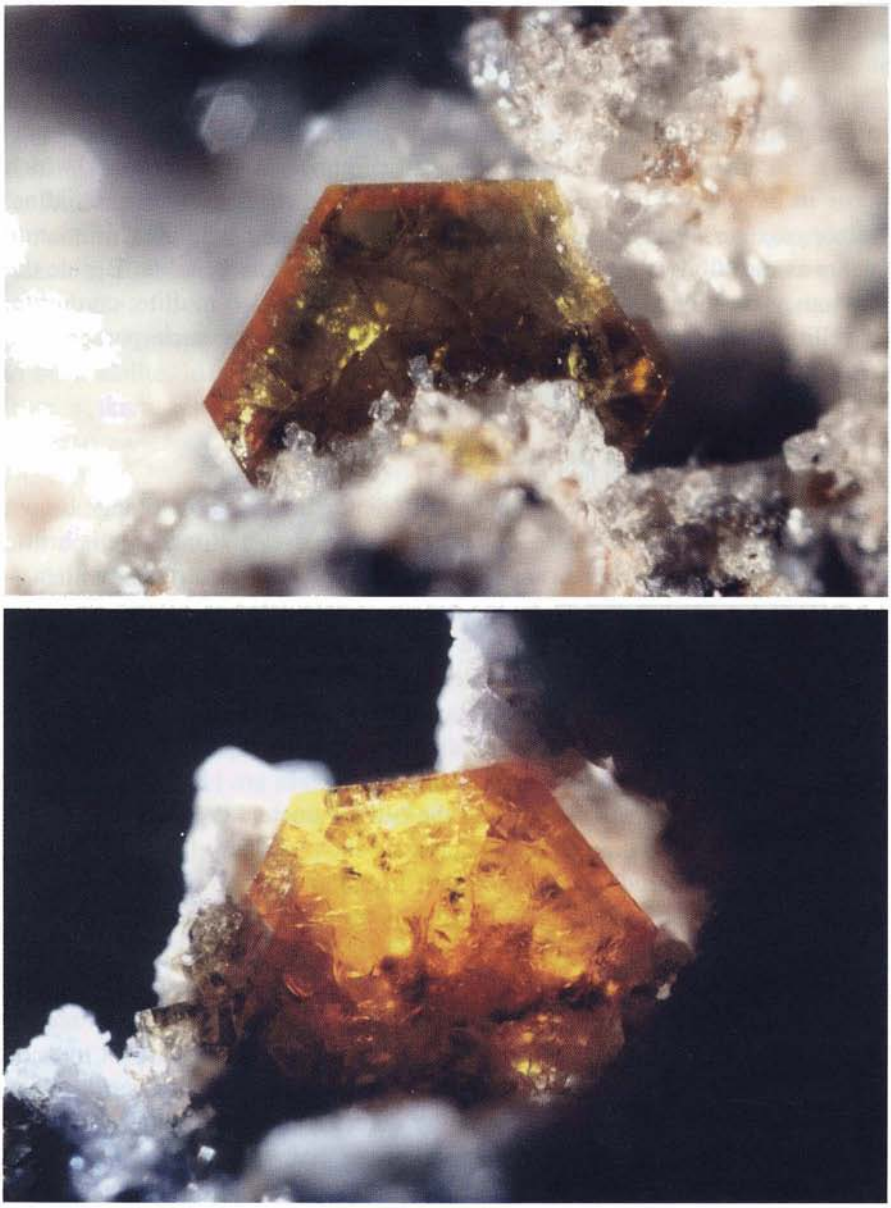

Fig. 1. Two microphotographs of almarudite from the Bellerberg, Eifel area (crystal diameter about 1.5 mm). Photography by courtesy of E. VAN DER MEERSCHE, Gent.

as excellent. No fluorescence under both short- and long-wave ultraviolet light was observed for rondorfite, almarudite and iron-rich wadalite.

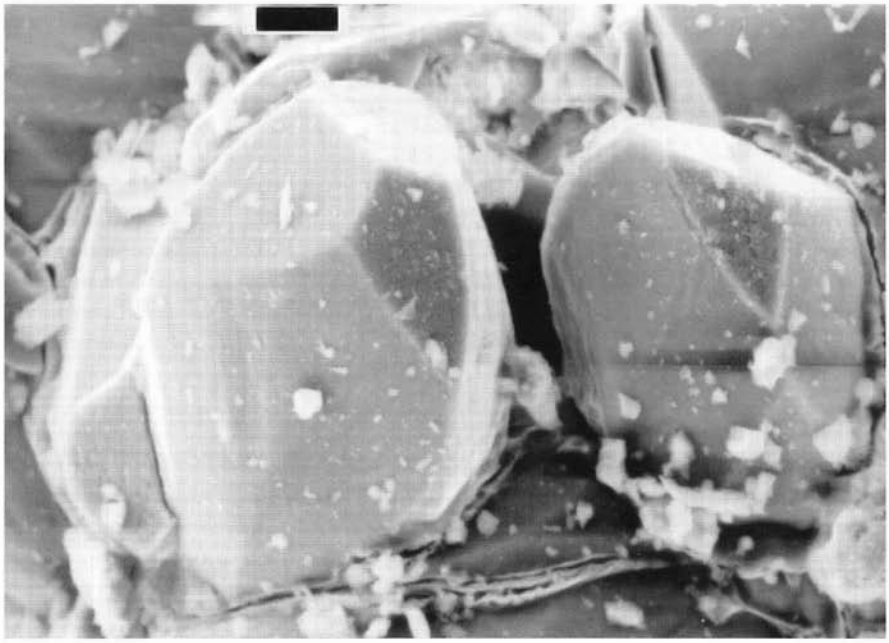

Fig. 2. SEM micrograph of iron-rich wadalite from the Bellerberg, Eifel area (scale bar at top: 10 μm).

Chemical composition

The chemical compositions of the investigated minerals were established by means of quantitative electron microprobe (EMP) analyses, which were performed on a Cameca SX100 microprobe at 15 kV and 20 nA sample current and measurement time of 20 s per element. The used standards are listed in the respective tables. According to the general formula $M_8T2^{[4]}[T1O_4]_4X_2$ the empirical formula of rondorfite obtained from the chemical analyses (Table 1) and calculated on the basis of O = 16+1 can be given as $(Ca_{7.98}Na_{0.02})(Mg_{0.87}Fe_{0.06}Al_{0.06})^{[4]}[(Si_{3.98}Ti_{0.01})O_{16}](Cl_{1.92}OH_{0.08})$. By comparison to the ideal formula $Ca_8Mg[SiO_4]_4Cl_2$ the EMP analyses show a small substitution of Na for Ca, Fe^{2+} and Al for Mg, and OH for Cl. The measurements on several grains revealed almost no chemical variation or zoning. A sulphur content was near the detection limit (S < 0.05 wt.%). Neither rondorfite nor the intergrown $Ca_2SiO_4 \cdot 0.5H_2O$ phase contained any Sr or K.

The chemical composition of almarudite, given in Table 2, was established by means of EMP analyses, supplemented by LAM–ICP–MS analyses for lithium, beryllium and boron. Using the general formula of the milarite-type compounds $A^{[12]}B_2^{[9]}M_2^{[6]}T2_3^{[4]}[T1_{12}O_{30}]$, the empirical formula obtained from

Table 1. Electron microprobe analyses (n = 8) of rondorfite.

Constituent	Wt. %	Range	s.d.	Standard
Na_2O	0.07	0.05–0.09	0.02	albite
MgO	4.52	4.43–4.50	0.13	olivine-SC
CaO	57.05	56.98–57.11	0.05	wollastonite
FeO	0.54	0.49–0.62	0.04	wüstite syn.
Al_2O_3	0.40	0.37–0.43	0.02	corundum syn.
SiO_2	30.51	30.37–30.67	0.10	wollastonite
TiO_2	0.13	0.11–0.14	0.02	rutile syn.
Cl (–O≡Cl)	6.71	6.67–6.77	0.04	halite syn.
Total	99.93			

Table 2. Electron microprobe analyses (n = 7) of almarudite.

Constituent	Wt. %	Range	s.d.	Standard
Na_2O	0.66	0.35–1.01	0.22	albite
K_2O	4.05	3.63–4.26	0.17	orthoclase
BeO*	5.18	4.69–5.69	0.38	NBS 612
MgO	1.51	1.12–1.99	0.31	olivine-SC
CaO	0.12	0.09–0.49	0.13	periclase syn.
MnO	7.31	7.07–8.25	0.34	spessartine
FeO	4.48	4.23–4.95	0.20	wüstite syn.
ZnO	0.24	0.13–0.28	0.14	zincite syn.
Al_2O_3	4.09	3.87–4.17	0.12	corundum syn.
SiO_2	72.31	71.81–73.32	0.39	quartz
Total	99.95			

* By LAM-ICP-MS.

the chemical analyses and calculated on the basis of Si = 12 can be given as $K_{0.86}{}^{[12]}Na_{0.21}{}^{[9]}(Mn_{1.03}Fe_{0.62}Mg_{0.37}Zn_{0.03}Ca_{0.02})^{[6]}(Be_{2.09}Al_{0.79})^{[4]}[Si_{12}O_{30}]$, which can be simplified to $K(\square,Na)_2(Mn,Fe,Mg)_2(Be,Al)_3[Si_{12}O_{30}]$. It is worth to note that almarudite contains almost no calcium, which is different to milarite. Lithium, i.e. the sugilite component $KNa_2(Fe,Mn,Al)_2Li_3[Si_{12}O_{30}]$, was in the range of 35–82 ppm, and for boron values from 57 up to 192 ppm were observed. As indicated by the optical observations the zoning of the investigated crystals is due to chemical variations on the octahedrally coordinated site following a Mg ↔ Mn substitution.

With respect to the general formula $M_{12}[T_{14}O_{32}]X_6$ the analytical results of the iron-rich wadalite given in Table 3, lead to the chemical composition $Ca_{12.00}[(Al_{7.32}Si_{4.24}Fe_{1.64}Mg_{0.68}Ti_{0.15})O_{31.97}]Cl_{5.78}$, based on the sum of cations

Table 3. Electron microprobe analyses (n = 11) of Fe-rich wadalite.

Constituent	Wt.%	Range	s.d.	Standard
MgO	1.68	1.57–1.74	0.11	olivine-SC
CaO	41.55	41.46–41.67	0.06	wollastonite
Al_2O_3	23.06	22.51–23.45	0.33	corundum syn.
Fe_2O_3	8.06	7.86–8.35	0.12	wüstite syn.
SiO_2	15.66	15.33–15.94	0.28	wollastonite
TiO_2	0.72	0.69–0.78	0.03	rutile syn.
Cl (–O≡Cl)	9.79	9.70–9.85	0.04	halite syn.
Total	100.52			

= 26, which can be simplified to $Ca_{12}[(Al_8Si_4Fe_2)O_{32}]Cl_6$. The crystals studied showed a distinct compositional zoning at their outermost rim: the Mg and Si contents increase toward the rim, with a simultaneous decrease of the Al and Fe^{3+} contents following the charge-balanced relationship $Mg^{2+} + Si^{4+} \leftrightarrow Al^{3+} + Fe^{3+}$. The corresponding formula can be given as $Ca_{12.00}[(Al_{7.10}Si_{4.54}Fe_{1.34}Mg_{0.87}Ti_{0.15})O_{31.99}]Cl_{5.84}$. Despite the occurrence of fluorite and cuspidine in this assemblage, no F was detectable in the investigated crystals. Na_2O was present with < 0.05 wt.%. Due to the structural characteristic of the mayenite-type compounds with two crystallochemically comparable *T*-sites the derived structural formula for wadalite is covered in the discussion section below.

X-ray powder investigation

The observed X-ray powder diffraction data for holotype rondorfite and almarudite were obtained with a 114.59 mm Gandolfi camera (GANDOLFI 1964) in asymmetric setting (STRAUMANIS & JEVINŠ 1936) using Ni-filtered CuK_α radiation and are given in Tables 4 and 5. The data were corrected for film shrinkage, the I/I_{obs} values were estimated visually, the *hkl* assignment was based on theoretical powder patterns calculated from the refined structure models (FISCHER et al. 1993), and the cell parameters of the powder data were refined using NBS*AIDS83 (MIGHELL et al. 1981). For the Fe-rich wadalite an in-house modified capillary measurement device based on a Philips X'Pert MPD diffractometer equipped with a germanium monochromator and a position sensitive detector was used. A list of the X-ray powder diffraction data with the most important values for identification purposes are summarised in Table 6.

The refined cubic cell parameter for rondorfite from the X-ray powder data is a = 15.087(2) Å and is, within the standard deviation, in good agreement with the result of the single-crystal measurement with a = 15.0850(3) Å. The

Table 4. X-ray powder diffraction data of rondorfite.

I/I_{obs}	I/I_{calc}*	d_{obs}	d_{calc}**	h	k	l
20	4.3	8.669	8.7102	1	1	1
15	6.4	5.323	5.3339	2	2	0
20	10.0	4.545	4.5488	3	1	1
5	4.4	4.365	4.3551	2	2	2
5	4.0	3.767	3.7716	4	0	0
15	6.0	3.074	3.0795	4	2	2
40	17.5	2.901	2.9034	5	1	1
100	100.0	2.666	2.6669	4	4	0
30	13.5	2.549	2.5501	5	3	1
10	4.5	2.383	2.3854	6	2	0
15	5.9	2.302	2.3007	5	3	3
15	6.1	2.272	2.2744	6	2	2
20	9.0	2.111	2.1125	5	5	1
30	14.7	1.964	1.9641	5	5	3
30	13.3	1.885	1.8858	8	0	0
5	3.3	1.844	1.8431	7	3	3
30	10.7	1.777	1.7780	8	2	2
20	9.3	1.742	1.7420	5	5	5
5	2.8	1.688	1.6867	8	4	0
5	1.9	1.580	1.5815	9	3	1
50	24.6	1.540	1.5398	8	4	4
30	12.7	1.459	1.4585	9	5	1
15	5.5	1.333	1.3335	8	8	0
10	4.4	1.224	1.2237	10	6	4
20	6.6	1.193	1.1927	12	4	0
20	6.0	1.154	1.1537	9	9	3
10	3.6	1.020	1.0195	13	5	5
10	4.2	1.008	1.0080	12	8	4

Notes: Gandolfi camera, diameter 114.59 mm, CuK_α, Ni-filter, 20 h; I/I_{obs} estimated visually.

* I/I_{calc} and $h\,k\,l$ indexing based on a theoretical powder pattern calculated from the refined single-crystal structure.

** Derived from the refined cell parameters of the powder data with $a = 15.087(2)$ Å. The results of a capillary measurement from a different sample are registered with ICDD entry 49–1855.

results for a capillary measurement of a different rondorfite sample are registered with ICDD entry 49–1855. The refinement of these data revealed a slightly reduced cell parameter with $a = 15.0794(1)$ Å. The hexagonal cell parameters for almarudite are $a = 9.995(1)$ and $c = 14.093(2)$ Å; both are well

Table 5. X-ray powder diffraction data of almarudite.

I/I_{obs}	I/I_{calc}*	d_{obs}	d_{calc}**	h	k	l
40	14.1	7.047	7.0464	0	0	2
25	4.7	5.467	5.4646	1	0	2
40	52.2	5.000	4.9974	1	1	0
30	12.3	4.331	4.3279	2	0	0
80	38.8	4.076	4.0763	1	1	2
25	22.5	3.691	3.6879	2	0	2
40	28.3	3.522	3.5232	0	0	4
30	5.0	3.266	3.2716	2	1	0
	10.4		3.2632	1	0	4
90	100.0	3.187	3.1868	2	1	1
5	2.1	2.967	2.9674	2	1	2
100	6.3	2.882	2.8853	3	0	0
	48.4		2.8795	1	1	4
50	32.6	2.732	2.7323	2	0	4
30	10.3	2.687	2.6847	2	1	3
20	4.3	2.498	2.4987	2	2	0
10	10.0	2.400	2.4007	3	1	0
20	2.7	2.365	2.3666	3	1	1
	2.4		2.3550	2	2	2
15	6.7	2.139	2.1377	3	1	3
30	7.2	1.983	1.9839	3	1	4
15	5.8	1.890	1.8889	4	1	0
15	8.9	1.873	1.8721	4	1	1
40	17.6	1.826	1.8276	3	1	5
	4.1		1.8244	4	1	2
5	6.1	1.762	1.7616	0	0	8
20	8.6	1.712	1.7114	2	2	6
20	2.6	1.665	1.6658	3	3	0
	3.9		1.6647	4	1	4
5	4.7	1.569	1.5691	4	1	5
30	4.7	1.506	1.5060	3	3	4
15	5.0	1.440	1.4398	2	2	8
30	6.0	1.414	1.4148	4	2	5
	4.1		1.4133	6	0	2
10	8.3	1.386	1.3860	5	2	0
10	3.0	1.356	1.3564	1	1	10
10	4.3	1.335	1.3351	6	0	4
20	7.5	1.312	1.3115	3	1	9
30	2.0	1.195	1.1954	6	1	5
	4.5		1.1937	5	2	6
10	4.4	1.178	1.7775	4	4	4
20	4.4	1.089	1.0893	5	2	8

Notes: Gandolfi camera, diameter 114.59 mm, CuK_α, Ni-filter, 16 h; I/I_{obs} estimated visually.

* I/I_{calc} and hkl indexing based on a theoretical powder pattern calculated from the refined single-crystal structure.

** Derived from the refined cell parameters of the powder data with $a = 9.995\,(1)$ and $c = 14.093\,(2)$ Å.

Table 6. X-ray powder diffraction data of Fe-rich wadalite.

I/I_{obs}	I/I_{calc}*	d_{obs}	d_{calc}**	h	k	l
15	14.0	4.912	4.9130	2	1	1
11	10.2	3.215	3.2163	3	2	1
48	36.5	3.008	3.0086	4	0	0
100	100.0	2.691	2.6909	4	2	0
9	6.5	2.565	2.5657	3	3	2
46	39.1	2.456	2.4565	4	2	2
21	23.1	2.360	2.3601	5	1	0
19	14.9	2.197	2.1971	5	2	1
10	6.7	1.952	1.9522	5	3	2
13	12.1	1.737	1.7370	4	4	4
8	4.8	1.702	1.7019	7	1	0
34	26.9	1.669	1.6689	6	4	0
8	4.7	1.637	1.6377	5	5	2
31	28.6	1.608	1.6081	6	4	2
14	7.2	1.504	1.5043	8	0	0
8	6.0	1.481	1.4813	7	4	1
9	5.3	1.399	1.3990	7	5	0, 7 4 3
4	2.2	1.363	1.3626	7	5	2
9	4.9	1.345	1.3455	8	4	0
16	10.6	1.313	1.3130	8	4	2
9	4.7	1.283	1.2829	6	6	4
7	3.8	1.215	1.2156	9	4	1, 8 5 3
17	10.8	1.117	1.1174	8	6	4, 10 4 0

Notes: Philips X'PertMPD, CuK_{α_1}, Ge monochromator, 36 h.

* I/I_{calc} and $h\,k\,l$ indexing based on a theoretical powder pattern calculated from the refined single-crystal structure.

** Derived from the refined cell parameters of the powder data with a = 12.0343 (2) Å. The complete results of this capillary measurement are registered with ICDD entry 49–1856.

comparable to the results of the single-crystal data collection (a = 9.997(1), c = 14.090(1) Å). The cubic cell parameter for the Fe-rich wadalite from the capillary measurement is a = 12.0343(2) Å and a = 12.0431(6) Å from the single-crystal dataset. Due to the higher accuracy, for rondorfite and almarudite the cell parameters obtained from the single-crystal data were used; for wadalite, however, the value from the powder data refinement was applied in the single-crystal structure refinements and the consecutive crystallochemical calculations.

Table 7. Single-crystal X-ray data collection and structure refinement.

	rondorfite	almarudite	Fe-rich wadalite
Space group	$Fd\bar{3}$, no. 203, 2nd	$P6/mmc$, no. 192	$I\bar{4}3d$, no. 220
Z	8	2	2
a [Å]	15.0850 (3)	9.997 (1)	12.0343 (2)*
c [Å]		14.090 (1)	
V [Å^3]	3432.7 (1)	1219.5 (2)	1742.9 (1)
D_{calc} [gcm^{-3}]	3.034	2.720	3.105
Formula weight	784.1	998.7	1629.7
Wavelength [Å]	0.71073	0.71073	0.71073
μ MoK_α [cm^{-1}]	3.202	1.861	3.390
Crystal size [mm^3]	0.11 × 0.13 × 0.14	0.10 × 0.13 × 0.17	0.13 × 0.14 × 0.15
Transmission factors	0.593–0.903	0.737–0.836	0.630–0.667
Absorption correction	ψ-scan	multi-scan	ψ-scan
θ range [°]	2.34–39.85	3.73–30.97	4.15–42.43
h, k, l ranges	$-22 < h < +27$	$-14 < h < +14$	$-21 < h < +22$
	$0 < k < +27$	$-14 < k < +14$	$-22 < k < +9$
	$-27 < l < +27$	$-20 < l < +20$	$-22 < l < +22$
No. of total reflections	7577	11972	6106
No. of unique F^2_o (n)	895 (R_{int} 7.19 %)	673 (R_{int} 2.55 %)	980 (R_{int} 5.25 %)
No. of $F^2_o > 4\sigma$ (F^2_o)	668	630	844
No. of parameters (p)	31	52	31
No. of constraints	2	2	2
$R1$, $R1 > 4\sigma$ (F^2_o)	4.59, 2.31 %	2.05, 1.85 %	3.64, 2.38 %
w$R2$, w$R2 > 4\sigma$ (F^2_o)	4.79, 4.42 %	4.54, 4.48 %	4.81, 4.61 %
GoF (s), Δ_{max}/σ	0.950, 0.001	1.127, 0.001	1.018, 0.083
Δ eÅ^{-3}	−0.63/+0.57	−0.27/+0.26	−0.41/+0.58
equipment	Stoe AED2	Nonius KappaCCD	Stoe AED2

$R1 = \Sigma\big|\,|F_o| - |F_c|\,\big|/\Sigma|F_o|$, w$R2 = [\Sigma[w(F_o^2 - F_c^2)^2]/\Sigma\, w(F_o^2)^2]^{1/2}$, s $= [\Sigma[w(F_o^2 - F_c^2)^2]/(n\text{-}p)]^{1/2}$, w $= 1/[\sigma^2 F_o^2 + (a * P)2 + b * P]$ with P $= [\max(F_o^2,0) + 2 * F_c^2]/3$ and for a, b: 0.027, 0.000 (rondorfite); 0.021, 0.610 (almarudite); 0.025, 0.000 (Fe-rich wadalite).

* Value obtained from Rietveld refinement of X-ray powder data.

Single-crystal X-ray diffraction

The single-crystal data for rondorfite and the Fe-rich wadalite were collected in 2θ/ω-scan mode using MoK_α radiation on a Stoe AED2 four-circle diffractometer equipped with a primary graphite monochromator and a scintillation counter. The data collection was monitored using three standard reflections measured every 2 h and for the absorption corrections ψ-scans were applied. For almarudite a Nonius Mach3 goniometer with a CCD area detector using

Table 8. Structural parameters for rondorfite (e.s.d.s in parentheses).

Site	Atom	CN	M	W	x	y	z	U_{eq}	s.o.f.
M1	Ca	[6]	16	*d*	1/2	1/2	1/2	0.00710 (7)	1.000
M2	Ca	[6+2]	48	*f*	0.34060 (2)	1/8	1/8	0.00865 (6)	1.000
T2	Mg	[4]	8	*a*	1/8	1/8	1/8	0.0061 (2)	0.912 (3)*
	Fe								0.028 (3)*
	Al								0.060*
T1	Si	[4]	32	*e*	0.25943 (2)	x	x	0.00521 (8)	1.000
O1	O		32	*e*	0.19679 (5)	x	x	0.0121 (2)	1.000
O2	O		96	*g*	0.60157 (5)	0.29601 (5)	0.01994 (5)	0.0088 (1)	1.000
X	Cl		16	*c*	0	0	0	0.0118 (1)	0.929 (3)**
	O								0.071 (3)**

Site	U_{11}	U_{22}	U_{33}	U_{23}	U_{13}	U_{12}
M1	0.00710 (7)	U_{11}	U_{11}	0.00106 (8)	U_{23}	U_{23}
M2	0.0089 (1)	U_{11}	U_{11}	−0.00155 (8)	0	0
T2	0.0061 (2)	U_{11}	U_{11}	0	0	0
T1	0.00521 (8)	U_{11}	U_{11}	0.00018 (7)	U_{23}	U_{23}
O1	0.0121 (2)	U_{11}	U_{11}	−0.0031 (3)	U_{23}	U_{23}
O2	0.0065 (3)	0.0095 (3)	0.0105 (3)	−0.0015 (2)	0.0003 (2)	−0.0012 (2)
X	0.0118 (1)	U_{11}	U_{11}	0.0000 (1)	U_{23}	U_{23}

CN: coordination number, M: site multiplicity, W: Wyckoff letter, U_{eq}: equivalent isotropic displacement factor according to FISCHER & TILLMANNS (1988), s.o.f.: refined site occupation factor. The anisotropic displacement factors (U_{ij}) are defined as exp $[-2\pi^2 \Sigma_{i=1} \Sigma_{j=1} U_{ij} a_i * a_j * h_i h_j]$.

* Al was fixed to the results of the chemical analysis and the remaining sum of the s.o.f.'s was constrained to be 0.940.

** The sum of the s.o.f.s was constrained to be 1.000.

MoK_α radiation, a primary graphite monochromator, and a 0.3 mm capillary optics collimator was chosen for the single-crystal data collection. For absorption correction the multi-scan approach was applied (OTWINOWSKI & MINOR 1997). The structures of all three minerals were refined on F^2 using SHELXL (release 2) of the SHELX–97 programs (SHELDRICK 1997) and the complex scattering factors of the ionic atoms (WILSON & PRINCE 1999). For the bond-valence calculations the parameters of BRESE & O'KEEFFE (1991) for metal – oxygen bonds, and the parameters of BROWN (1996; updated values www.ccp14.ac.uk/ccp/web-mirrors/i_d_brown) for metal – chlorine bonds were used.

A total of 7577 reflections, assuming a primitive cubic cell, were collected in the θ range 2.34 – 39.85° for rondorfite, which were reduced to a unique da-

Table 9. Selected interatomic distances [Å] and angles [°] for rondorfite and its synthetic analogue (e.s.d.s in parentheses).

	rondorfite	synthetic*
M1–O2 × 6	2.3634 (8)	2.365
M2–O2 × 2	2.3585 (8)	2.362
–O2 × 2	2.4955 (8)	2.486
–O1 × 2	2.6555 (3)	2.655
–*X* × 2	2.9965 (2)	2.994
<*M2*–(O, *X*)>	2.627	2.624
T2–O1 × 4	1.876 (1)	1.860
T1–O2 × 3	1.6298 (7)	1.621
–O1	1.637 (1)	1.641
<*T1*–O>	1.632	1.626
O1–*T2*–O1 × 6	109.47	109.5
O2–*T1*–O2 × 3	113.86 (2)	113.8
O2–*T1*–O1 × 3	104.61 (3)	104.7

* YE et al. (1987).

taset of 895 observations (R_{int} 7.19 %) and 668 with $F^2_o > 4\sigma$ (F^2_o). Evaluation of the intensities using XPREP (SIEMENS 1990) gave a clear indication for space group $Fd\bar{3}$ and not for $Fd\bar{3}m$ as reported by YE et al. (1987) and the refinement was started with the positional parameters of VON LAMPE et al. (1986). For the refinement of the mixed occupancy of Mg, Fe, and Al on the tetrahedrally coordinated *T2*-site the Al content was fixed according to the chemical analysis and Mg and Fe were constrained to the remaining sum. Also for the *X*-site the chlorine and oxygen content were refined using one constraint on the sum of the site occupation factors. The final refinement converged at $R1 = 2.31\,\%$ ($wR2 = 4.42\,\%$) and the maximum peaks in the final difference-Fourier maps were 0.57 and $-0.63\,e\text{Å}^{-3}$, respectively. Further details of the data collection, the structure refinement and other relevant crystallographic data for rondorfite are summarised in Table 7, the final positional and displacement parameters are given in Table 8, and selected bond distances and angles in Table 9.

Single-crystal X-ray intensity data for almarudite were collected with a CCD area detector. A whole sphere up to 30.97° θ was collected using two sets of ψ-scans and five sets of ω-scans with a total of 693 frames of 1.5° rotation width, 2 × 120 s exposure time/frame, and a crystal – detector distance of 35 mm. The total of 11972 reflections, assuming a cell in *P*1, were reduced to a unique dataset of 673 observations (R_{int} 2.55 %) and 630 with $F^2_o > 4\sigma$ (F^2_o).

Table 10. Structural parameters for almarudite (e.s.d.s in parentheses).

Site	Atom	CN	M	W	x	y	z	U_{eq}	s.o.f.
A	K	[12]	2	a	0	0	1/4	0.0251 (3)	0.928 (5)
B	Na	[9]	8	h	1/3	2/3	0.025 (1)	0.009 (5)	0.050 (4)
M	Mn	[6]	4	c	1/3	2/3	1/4	0.0106 (2)	0.529 (3)*
	Fe								0.310*
	Mg								0.161 (3)*
T2	Be	[4]	6	f	1/2	0	1/4	0.0114 (4)	0.738 (3)**
	Al								0.262 (3)**
T1	Si	[4]	24	m	0.09503 (3)	0.35169 (3)	0.10857 (2)	0.0085 (1)	1.000
O1	O		12	l	0.1130 (2)	0.4089 (2)	0	0.0221 (3)	1.000
O2	O		24	m	0.2077 (1)	0.2827 (1)	0.12747 (7)	0.0241 (2)	1.000
O3	O		24	m	0.12912 (9)	0.48752 (9)	0.18076 (5)	0.0150 (2)	1.000

Site	U_{11}	U_{22}	U_{33}	U_{23}	U_{13}	U_{12}
A	0.0243 (4)	U_{11}	0.0268 (6)	0	0	$U_{11}\times0.5$
B	0.002 (4)	U_{11}	0.02 (1)	0	0	$U_{11}\times0.5$
M	0.0109 (2)	U_{11}	0.0099 (2)	0	0	$U_{11}\times0.5$
T2	0.0130 (5)	0.0104 (7)	0.0099 (6)	0	0	$U_{11}\times0.5$
T1	0.0090 (2)	0.0104 (2)	0.0066 (2)	−0.00154 (9)	−0.00035 (9)	0.00521 (11)
O1	0.0373 (7)	0.0206 (6)	0.0074 (5)	0	0	0.0138 (6)
O2	0.0273 (5)	0.0373 (6)	0.0216 (4)	−0.0064 (4)	−0.0036 (4)	0.0265 (5)
O3	0.0236 (4)	0.0156 (4)	0.0105 (4)	−0.0040 (3)	−0.0028 (3)	0.0132 (3)

CN: coordination number, M: site multiplicity, W: Wyckoff letter, U_{eq}: equivalent isotropic displacement factor according to FISCHER & TILLMANNS (1988), s.o.f.: refined site occupation factor. The anisotropic displacement factors (U_{ij}) are defined as exp $[-2\pi^2 \Sigma_{i=1} \Sigma_{j=1} U_{ij} a_i * a_j * h_i h_j]$.

* Fe was fixed to the results of the chemical analysis and the remaining sum of the s.o.f.'s was constrained to be 0.690.

** The sum of the s.o.f.s was constrained to be 1.000.

As reported by ARMBRUSTER et al. (1989) for the milarite from Val Giuf, also in the case of almarudite the forbidden reflection (0.0.15) was observed with an I/σ of 5.4. Careful inspection of the respective frames, however, clearly revealed this data inconsistency as an artefact during the integration process of the used Denzo algorithm (OTWINOWSKI & MINOR 1997). Beside that, no significant violations of space group symmetry *P6/mcc* were observed. The refinement was started with the positional parameters of the natural milarite of ARMBRUSTER et al. (1989). Subsequent difference-Fourier maps, however, gave a clear indication for a partially occupied *B*-site. For the refinement of the mixed occupancy of Mn, Fe, and Mg on the octahedrally coordinated

Table 11. Selected interatomic distances [Å] and angles [°] for almarudite and related milarites (e.s.d.s in parentheses).

	almarudite	milarite*	1100 K**		almarudite	1100 K**
A–O2×12	3.068 (1)	3.008–3.022	3.015			
B–O1×3	2.437 (2)	2.774–2.799	2.718	O1–*B*–O1×3	118.0 (2)	120.00
–O3×3	2.93 (1)	2.798–3.045	3.286	O3–*B*–O3×3	69.6 (3)	68.51
–O3′×3	3.48 (1)		3.286	O3′–*B*–O3′×3	57.4 (2)	68.51
–B′	0.69 (3)	0.69–1.39				
M–O3×6	2.161 (1)	2.327–2.370	2.341	O3–*M*–O3×3	70.21 (4)	67.10
				O3–*M*–O3×3	88.28 (4)	84.92
				O3–*M*–O3×6	101.21 (3)	104.36
				O3–*M*–O3×3	168.47 (4)	169.02
T2–O3×4	1.671 (1)	1.636–1.675	1.660	O3–*T2*–O3×2	96.06 (5)	102.41
				O3–*T2*–O3×2	108.59 (5)	109.37
				O3–*T2*–O3×2	125.14 (6)	116.96
T1–O3	1.591 (1)	1.588–1.609	1.589	O2–*T1*–O2	104.01 (8)	104.43
–O2	1.608 (1)	1.592–1.621	1.618	O1–*T1*–O2	109.35 (6)	109.54
–O2	1.610 (1)	1.617–1.620	1.619	O2–*T1*–O3	109.73 (5)	111.04
–O1	1.612 (1)	1.614–1.618	1.616	O1–*T1*–O2	110.81 (6)	110.48
				O2–*T1*–O3	111.26 (5)	110.77
				O1–*T1*–O3	111.45 (6)	110.43
				T1–O1–*T1*	143.35 (9)	148.03
				T1–O2–*T1*	156.45 (8)	154.75
				T1–O3–*T2*	126.36 (5)	129.23
				T1–O3–*M*	134.93 (5)	133.79
				T2–O3–*M*	96.86 (4)	95.25

* Hawthorne et al. (1991): value ranges for several milarites.

** Armbruster et al. (1989): milarite heated at 1100 K.

M-site, the Fe content was fixed according to the chemical analysis and Mn and Mg were constrained to the remaining sum. For the *T2*-site Be and Al were constrained to a full occupancy. The final refinement converged at $R1 = 1.85\,\%$ ($wR2 = 4.48\,\%$) and the maximum peaks in the final difference-Fourier maps were 0.26 and $-0.27\,e\text{Å}^{-3}$, respectively. It is worth to note that no significant electron densities were observed for the *C*-site. Further details of the data collection, the structure refinement and other relevant crystallographic data for almarudite are summarised in Table 7, the final positional and displacement parameters are given in Table 10, and selected bond distances and angles in Table 11.

Table 12. Structural parameters for Fe-rich wadalite from the Bellerberg (e. s. d.s in parentheses).

Site	Atom	CN	M	W	x	y	z	U_{eq}	s. o. f.
M	Ca	[6+1]	24	d	0.10461 (3)	0	1/4	0.00965 (7)	1.000
T2	Si	[4]	16	c	0.23312 (2)	x	x	0.0058 (1)	0.485 (5)*
	Al								0.331 (3)*
	Fe								0.165 (3)*
	Ti								0.019*
T1	Al	[4]	12	a	3/8	0	1/4	0.0074 (1)	0.788 (4)*
	Si								0.050 (6)*
	Fe								0.049 (5)*
	Mg								0.113*
O1	O1		16	c	0.06319 (9)	x	x	0.0142 (3)	1.000
O2	O2		48	e	0.03132 (8)	0.05061 (9)	0.64877 (9)	0.0130 (2)	1.000
X	Cl		12	b	7/8	0	1/4	0.0206 (2)	0.949 (4)

Site	U_{11}	U_{22}	U_{33}	U_{23}	U_{13}	U_{12}
M	0.00924 (12)	0.00832 (12)	0.01138 (13)	0.00175 (11)	0	0
T2	0.00583 (11)	U_{11}	U_{11}	0.00034 (8)	U_{23}	U_{23}
T1	0.0057 (2)	0.00820 (16)	U_{22}	0	0	0
O1	0.0142 (3)	U_{11}	U_{11}	0.0033 (3)	U_{23}	U_{23}
O2	0.0130 (4)	0.0108 (4)	0.0152 (4)	0.0015 (3)	−0.0020 (3)	0.0011 (3)
X	0.0085 (3)	0.0267 (3)	U_{22}	0	0	0

CN: coordination number, M: site multiplicity, W: Wyckoff letter, U_{eq}: equivalent isotropic displacement factor according to FISCHER & TILLMANNS (1988), s. o. f.: refined site occupation factor. The anisotropic displacement factors (U_{ij}) are defined as exp $[-2\pi^2 \Sigma_{i=1} \Sigma_{j=1} U_{ij} a_i * a_j * h_i h_j]$.

* Ti and Mg were fixed to the results of the chemical analysis and the remaining s. o. f.s were constrained to a sum of 1.000.

For the Fe-rich wadalite a total of 6106 reflections, assuming a primitive cubic cell, were collected in the θ range 4.15–42.43°, which were reduced to a unique dataset of 980 observations (R_{int} 5.25 %) and 884 with $F^2_o > 4\sigma (F^2_o)$. The mineral crystallises in $I\bar{4}3d$ and the refinement was started with the positional parameters of TSUKIMURA et al. (1993); however, the labelling of the crystallographic sites, which is not consistent in the literature, was set according to common usage, i.e. *T1, T2* and O1, O2 according to their multiplicity, and *X* for the charge compensating anion. For the refinement of the mixed occupancy of Al, Si, and Fe on the tetrahedrally coordinated *T1* and *T2*-site the Mg and Ti content were fixed according to the chemical analysis and Al, Si, and Fe were constrained to the remaining sum to give a full occupancy. The

Table 13. Selected interatomic distances [Å] for Fe-rich wadalite from the Bellerberg and related compounds.

	this study	wadalite*	synthetic**
M–O1×2	2.4250 (9)	2.422 (9)	2.399 (6)
–O2×2	2.429 (1)	2.429 (8)	2.426 (3)
–O2×2	2.525 (1)	2.515 (8)	2.509 (3)
–*X*	2.7632 (4)	2.752 (3)	2.767 (1)
<*M*–(O, *X*)>	2.503	2.498	2.491
T2–O1	1.669 (2)	1.657 (18)	1.705 (6)
–O2×3	1.738 (1)	1.729 (9)	1.718 (3)
<*T2*–O>	1.721	1.711	1.715
T1–O2×4	1.768 (1)	1.765 (8)	1.762 (3)
O2–*T2*–O2×3	99.76 (5)	99.7 (4)	100.3 (2)
O1–*T2*–O2×3	118.00 (4)	118.0 (3)	117.5 (2)
O2–*T1*–O2×3	100.77 (7)	100.3 (5)	101.3 (1)
O2–*T1*–O2×3	113.99 (4)	114.3 (3)	113.7 (1)
T1–O2–T2	139.61 (6)		

* Tsukimura et al. (1993).
** Feng et al. (1988).

chlorine content on the *X*-site was allowed to vary freely. The final refinement with a Flack parameter of 0.02(4) converged at $R1 = 2.38\,\%$ ($wR2 = 4.61\,\%$) and the maximum peaks in the final difference-Fourier maps were 0.58 and $-0.41\,e\text{Å}^{-3}$, respectively. Further details of the data collection, the structure refinement and other relevant crystallographic data for wadalite are summarised in Table 7, the final positional and displacement parameters are given in Table 12, and selected bond distances and angles in Table 13.

Results and discussion

Rondorfite

The structure of rondorfite is in good agreement with that of synthetic $Ca_8Mg[SiO_4]_4Cl_2$ determined by Ye et al. (1987), although a detailed evaluation of the collected single-crystal intensity data of rondorfite yielded the polar space group $Fd\bar{3}$ (no. 203) instead of $Fd\bar{3}m$ (no. 227) as reported by Ye et al. (1987) for a synthetic sample ($R = 7.3\,\%$). The single-crystal structure solution, however, of synthetic $Ca_8Mg[SiO_4]_4Cl_2$ in $Fd\bar{3}$ by von Lampe et al. (1986) is completely confirmed. The unit-cell parameter derived from the single-crystal data of rondorfite with $a = 15.0850(3)$ Å is slightly larger than that of the syn-

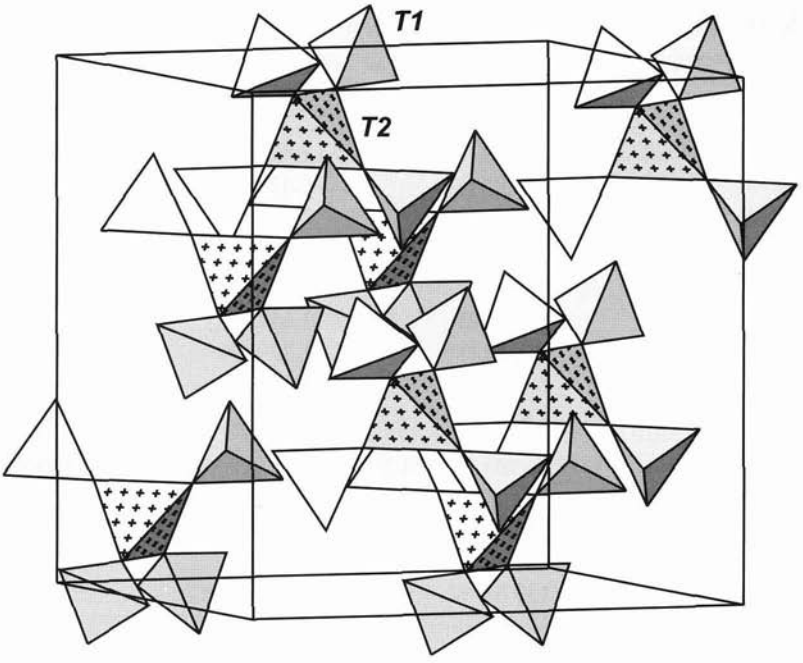

Fig. 3. Polyhedral view of the $Mg[SiO_4]_4$ pentamers (Mg: *T2*, Si: *T1*) in the unit cell of rondorfite. The Ca and Cl atoms are omitted for clarity. Drawing was performed using ATOMS (Dowty 1999).

thetic material characterised by Ye & Wang (1985) and Ye et al. (1987), a = 15.065(4) Å, but is almost identical to the value given by von Lampe et al. (1986) with a = 15.084 Å.

The atomic arrangement can be characterized by four isolated SiO_4 tetrahedra (*T1*), which are combined through O1 along [111] to a central *T2* cation, which is occupied by major Mg^{2+} and minor amounts of Al^{3+} and Fe^{2+} (Fig. 3). Due to the symmetry restrictions, this structural configuration is outstanding (i) in exhibiting a perfect tetrahedral coordination sphere of the *T2*-site, and (ii) in constraining a 180° *T1*–O1–*T2* intertetrahedral angle. Therefore, the *T1* – O1 distance exhibits with 1.637(1) Å a significant enlargement with respect to the *T1* – O2 distance (1.6298(7) Å) bridging to the calcium-dominated *M* site. The displacement factors of O1 (Table 8) are relatively high, which was also observed for the bridging oxygen in the straight *T*–O–*T* bonds in zunyite (Baur & Ohta 1982) and harkerite (Giuseppetti et al. 1977), thus reflecting different site occupations rather than a statistical disorder. Consequently, this structural unit can also be described as a magnesiosi-

licate Si_4MgO_{16} pentamer, a topological arrangement also found in the aluminosilicates zunyite (PAULING 1933, KAMB 1960) and harkerite (OSTROVSKAYA 1969, MACHIN & MIEHE 1976, GIUSEPPETTI et al. 1977), with bridging angles of 180° and 176°, respectively. Further discussions on these penta–aluminosilicates are given in LOUISNATHAN & GIBBS (1972), BAUR & OHTA (1982), and DIRKEN et al. (1995). The magnesiosilicate pentamers are connected via 12 M^{2+}–O bonds ($6\times$ *M1* – O2, $4\times$ *M2* – O2, $2\times$ *M2* – O1), plus six *M2* – *X* bonds, to form a three-dimensional framework. According to the single-crystal structure refinement, the site occupation factor (s.o.f.) of the *X*-site revealed an OH–for–Cl substitution of 7.1(3) % (Table 8), which is in good agreement with the EPM analyses. The bond-valence sums for the atoms in rondorfite taking into account the mixed occupancy of the *T2*-site (Mg, Fe, Al) are 2.05 (*M1*), 1.83 (*M2*), 2.46 (*T2*), 3.92 (*T1*), 2.04 (O1), 1.91 (O2) and 1.04 (*X*) valence units, which confirms the presence of considerable amounts of trivalent (Fe,Al) cations on the *T2*-site.

Almarudite

Almarudite is a new member of the milarite group (sometimes also designated as osumilite group). The various minerals of this group (Table 14) can be characterised by the general formula ($Z = 2$) $A_{1-x}{}^{[12]}B_{2-x}{}^{[9]}M_2{}^{[6]}T2_3{}^{[4]}[T1_{12}{}^{[4]}O_{30}]$, with A = (Na, K, □), B = (Na, H_2O, □), M = (Na, Mg, Al, Ca, Ti, Fe, Mn, Zr, Sn), *T2* = (Li, Be, B, Mg, Al, Fe, Zn), and *T1* = (Si, Al). The symmetry is hexagonal, or in the case of armenite, pseudo-hexagonal, and due to the chemical variability a wide range of the unit-cell parameters (a: 9.9 – 10.5 Å, c: 13.5 – 14.4 Å) is observed. Their structure consists of six-membered double rings of corner-linked $T1O_4$–tetrahedra, which are stacked along the c-axis and interconnected by the MO_6–octahedra and the $T2O_4$–tetrahedra. The *A* site is situated in the centre of the double rings; the *B* position, located in another void, is usually occupied by Na or H_2O and may be co-ordinated by the cation at the *A* site (Fig. 4 a+b). The bond-valence sums were calculated for the atoms in almarudite taking into account the mixed occupancies of the *M* (Mn, Fe, Mg) and *T2* (Be, Al) sites, and the partial occupancies of the *A* (K) and *B* (Na) sites (Table 10). The obtained values of 0.88 (*A* = K), 0.03 (*B* = Na), 2.03 (*M*), 2.34 (*T2*), 4.21 (*T1* = Si), 2.13 (O1), 2.16 (O2) and 2.02 (O3) valence units fully agree with the observed substitutions on the *M* and *T2* sites. The values also reflect that the *A* (K) and *B* (Na) sites are not fully occupied [a fully occupied *B* (Na) site would result in a severe oversaturation of the O1 site, with 2.42 valence units]. The value for the *T1* (= Si) site (4.21 valence units) appears somewhat high; although it could theoretically indicate a minor B-for-Si substitution, no significant B content was detectable in the chemical analyses.

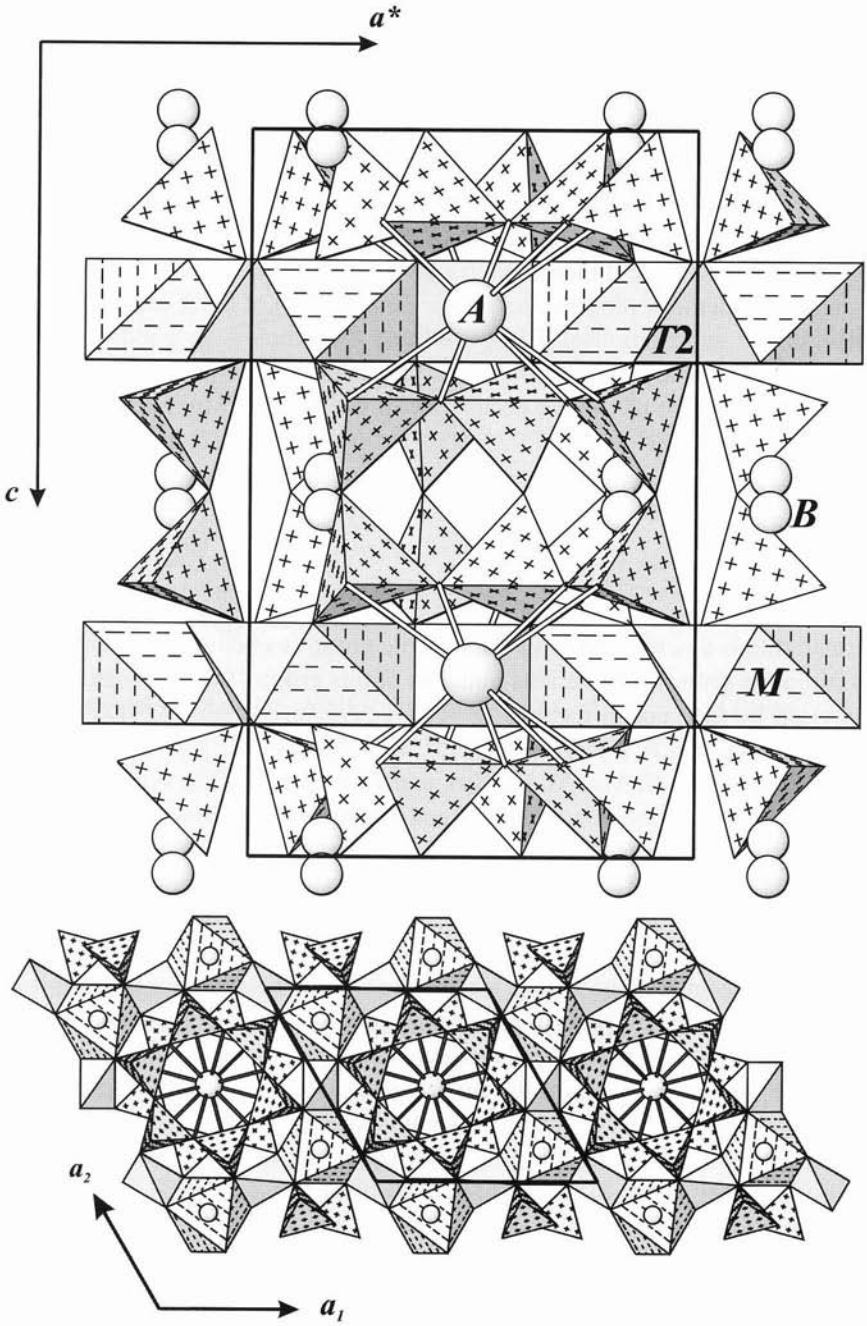

Fig. 4. Polyhedral view (K: *A*, Na: *B*, Mn: *M*, Be: *T2*, Si: *T1*) of almarudite (a) along [100] and (b) along [001]. Drawing was performed using ATOMS (Dowty 1999).

Table 14. Comparison of crystallographical data for almarudite and related $A^{[12]}B_2^{[9]}M_2^{[6]}T2_3^{[4]}[T1_{12}O_{30}]$-type minerals.

Ideal formula	Name	S. G.	a [Å]	c [Å]	V [Å^3]	D_x
$K(\square,Na)_2(Mn,Fe,Mg)_2(Be,Al)_3[Si_{12}O_{30}]$	*almarudite*	*P6/mcc*	9.997	14.090	1219.5	2.713
$K\square_2Ti_2Li_3[Si_{12}O_{30}]$	berezanskite (1)	$P6_3/mcc$	9.903	14.274	1212.3	2.674
$KNa_2(Fe,Mn,Al)_2Li_3[Si_{12}O_{30}]$	sugilite (2)	*P6/mcc*	10.009	14.006	1215.1	2.790
$K\square_2Na_2B_3[Si_{12}O_{30}]$	poudretteite (3)	*P6/mcc*	10.239	13.485	1224.3	2.535
$K\square_2Sn_2Li_3[Si_{12}O_{30}]$	brannockite (2)	*P6/mcc*	10.002	14.263	1235.7	2.995
$K(Na,\square)_2(Zr,Ti,Fe,Al)_2Li_3[Si_{12}O_{30}]$	sogdianite (4)	*P6/mcc*	10.053	14.211	1243.8	2.746
$\square\square_2(Fe,Mg)_2(Mg,Fe)_3[Si_{12}O_{30}]$	trattnerite*	*P6/mcc*	10.050	14.338	1254.1	2.690
$(Na,K)(Na,\square)_2Mg_2(Al,Mg,Fe)_3[(Si,Al)_{12}O_{30}]$	yagiite (5)	*P6/mcc*	10.09	14.29	1259.9	2.700
$K\square_2(Mg,Fe)_2(Al,Fe)_3[(Si,Al)_{12}O_{30}]$	osumilite-(Mg) (6)	*P6/mcc*	10.086	14.325	1262.0	2.582
$K(\square,Na)_2(Mg,Na)_2Mg_3[Si_{12}O_{30}]$	eifelite (7)	*P6/mcc*	10.137	14.223	1265.7	2.675
$K(Na,H_2O)_2(Mg,Fe)_2Mg_3[Si_{12}O_{30}]$	roedderite (8)	*P*–62*c*	10.141	14.286	1272.3	2.627
$(K,Na)\square_2(Fe,Mg)_2(Al,Fe)_3[(Si,Al)_{12}O_{30}]$	osumilite (6)	*P6/mcc*	10.145	14.289	1273.6	2.645
$K(K,\square)_2(Mg,Fe)_2(Fe,Mg)_3[Si_{12}O_{30}]$	merrihueite (9)	*P6/mcc*	10.16	14.32	1280.2	2.870
$K\square_2Mg_2(Mg,Fe)_3[Si_{12}O_{30}]$	chayesite (10)	*P6/mcc*	10.153	14.389	1284.5	2.680
$K(\square,H_2O)_2Ca_2(Be,Al)_3[Si_{12}O_{30}]$	milarite (11)	*P6/mcc*	10.396	13.781	1289.8	2.575
$K(K,Na,\square)_2(Mn,Zr)_2(Zn,Li)_3[Si_{12}O_{30}]$	dusmatovite (12)	$P6_3/mmc$	10.218	14.292	1292.3	2.987
$K(Na,\square)_2(Zr,Na)_2(Li,Mn,Zn)_3[Si_{12}O_{30}]$	darapiosite (13)	*P6/mcc*	10.32	14.39	1327.2	2.804
$K(K,\square)_2(Ca,Mn,Na)_2Zn_3[Si_{12}O_{30}]$	shibkovite (14)	*P6/mcc*	10.505	14.185	1355.7	2.900
$Ba(H_2O)_2Ca_2Al_3[Si_9Al_3O_{30}]$	armenite (15)	*Pnc*2	10.735**	13.874	1384.7**	2.754

Compilation from STRUNZ & NICKEL (2001), data partially corrected according to the following original publications: (1) Amer. Mineral. 83 (1998) 907, (2) Amer. Mineral. 73 (1988) 595, (3) Canad. Mineral. 25 (1987) 763, (4) Amer. Mineral. 84 (1999) 764, (5) Amer. Mineral. 54 (1969) 14, (6) Amer. Mineral. 73 (1988) 585, (7) Contrib. Mineral. Petrol. 82 (1983) 252, (8) Eur. J. Mineral. 1 (1989) 715, (9) Amer. Mineral. 50 (1965) 2096, (10) Amer. Mineral. 74 (1989) 1369, (11) Amer. Mineral. 76 (1991) 1836, (12) Amer. Mineral. 82 (1997) 430, (13) Amer. Mineral. 61 (1976) 1053, (14) Amer. Mineral. 85 (2000) 628, (15) Amer. Mineral. 84 (1999) 92.

* Pers. comm. F. WALTER, Graz.

** Pseudo-hexagonal values derived from the original orthorhombic cell.

The appearance, habit, and (partly) colour of almarudite are similar to those of roedderite, which also occurs at the Bellerberg locality (e.g., HENTSCHEL 1987, SCHÜLLER 1990), although roedderite crystals usually show paler colours. The association of almarudite with braunite may give some indication for the possible presence of a Mn-dominant milarite-group mineral, although detailed chemical investigations will be necessary for an unambiguous identification of almarudite. The empirical formula of almarudite, obtained from the chemical analyses and the single-crystal data structure refinement, can be given as $K_{0.86}{}^{[12]}Na_{0.21}{}^{[9]}(Mn_{1.03}Fe_{0.62}Mg_{0.37}Zn_{0.03}Ca_{0.02})^{[6]}(Be_{2.09}Al_{0.79})^{[4]}[Si_{12}O_{30}]$. All crystals analysed exhibit a distinct zoning due to chemical variations on the *M* site. This is in agreement with the observation of optically anomalous extinction and zoning at the outer rim.

The structure of almarudite is isotypic to that of milarite and the related compounds (Table 14). The *A* site is almost completely occupied by K (86 %), on the *B* site there are small amounts of Na (10 %), and for *T1* a fully occupied Si site can be assumed from the obtained results (Table 10). The chemistry of the *T2* site revealed a Be/(Be+Al) value of 0.738(3) which is well in the reported range for milarite (HAWTHORNE et al. 1991: 0.55 – 0.90). This holds also for the *T2*–O distance (Table 11) of 1.671(1) Å (*ibidem*: 1.636 – 1.675 Å). In contrast with the known milarite compositions, however, the *M* site of the new mineral is characterised by a lack of Ca and a dominance of Mn+Fe over Mg, as it is also reported for the milarite-group minerals sugilite and dusmatovite (Table 14). The Mn-bearing bulk chemistry of the almarudite-containing paragenesis is confirmed by the occurrence of braunite, previously reported for this locality (HENTSCHEL 1987, SCHÜLLER 1990). With respect to milarite the absence of Ca is responsible for a significant reduction (~5 %) of the unit-cell volume, therefore placing the new mineral in the lower volume range of this mineral group, which is usually dominated by the Li-bearing analogues (*cf.* Table 14). In order to verify a possible water content of almarudite, an additional single-crystal data refinement of intensity data measured after a thermal treatment at 1100 K for 12 h was performed, a procedure similar to that applied on natural milarite by ARMBRUSTER et al. (1989). No significant changes in unit-cell parameters or electron densities at the *A* and *B* sites between the room-temperature structure and the heat-treated structure were observed. Therefore, one can assume that no significant water content is present in almarudite, which is in agreement with the conditions of formation at high temperatures.

Fe-rich wadalite

The single-crystal structure refinement of the Fe-rich wadalite from the Bellerberg shows good agreement with the structural data (Table 13) reported for

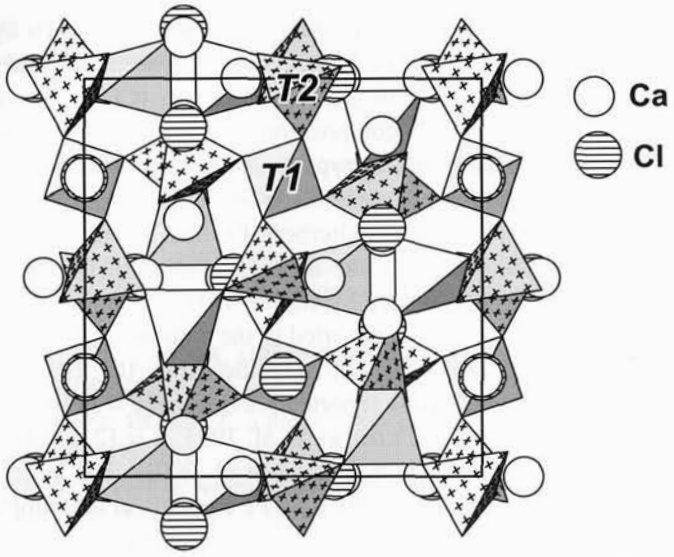

Fig. 5. The structure of iron-rich wadalite projected along [001], with the 4-connected *T1* (Al) and the 3-connected *T2* (Si) tetrahedra. Drawing was performed using ATOMS (DOWTY 1999).

type wadalite with the formula $(Ca_{11.76}Mg_{0.46})[(Al_{8.52}Fe_{0.92}Si_{4.00})O_{31.36}]Cl_{5.28}$ (TSUKIMURA et al. 1993) and for synthetic wadalite with the formula $Ca_{12}[(Al_{10.6}Si_{3.4})O_{32}]Cl_{5.4}$ (FENG et al. 1988). The structure (Fig. 5) contains two tetrahedrally coordinated sites, *T1* and *T2*, with a significant Al/Si disorder over both *T*-sites. In the case of the presently studied wadalite sample the single-crystal data refinement revealed electron densities of ~13 and ~16 e^- for the *T1*- and *T2*-site, respectively. As the *T1*-site exhibits with 1.768(1) Å for *T1* – O2 (Table 13) a significantly larger interatomic distance as compared to 1.721 Å for ⟨*T2* – O⟩, the Mg and Ti contents from the chemical analysis were assigned to the *T1*- and *T2*-site, respectively. The remaining occupancy was refined using two constraints by a simultaneous substitution of Al, Si and Fe at each site. The structural formula derived from the refined site occupation factors (Table 12) can be given as $Ca_{12.00}[(Si_{3.88}Al_{2.65}Fe_{1.32}Ti_{0.15})(Al_{4.73}Mg_{0.68}Si_{0.30}Fe_{0.29})O_{32}]Cl_{5.69}$, which is in good agreement with the results of the chemical analysis. This finding is also supported by the results of extensive bond-valence calculations, which showed that the *T1*- and *T2*-sites must be predominantly occupied by Al and Si, respectively. For the Ca site, the calculations yielded 1.94 valence units.

Synthetic wadalite with the formula $Ca_{12}[(Al_{9.9}Si_{4.05})O_{32}]Cl_{5.9}$ has also been characterised by FUJITA et al. (2001), albeit not by single-crystal methods; the

material of FUJITA et al. (2001) was prepared by reaction between hydrogrossular and HCl gas at 400–950 °C. Natural wadalite from Mexico with the composition $Ca_{11.98}[(Al_{6.70}Si_{5.40}Mg_{1.26}Fe^{3+}_{0.50})_{\Sigma 13.86}O_{32}]Cl_{5.86}$ was described by KANAZAWA et al. (1997); this composition is richer in Mg and has a lower $(Al+Fe^{3+}+Mg)/Si$ ratio than that of type wadalite, but contains less Al than the sample from the Bellerberg. A comparison of all mentioned analyses shows that, firstly, the material from the Bellerberg has the Fe-richest composition reported so far, and, secondly, that the ideal Cl content of 6 Cl pfu is never reached in both natural and synthetic samples. It is also noteworthy that not even minor Na or Sr contents were reported in the natural samples.

The refined unit-cell parameter of wadalite from the Bellerberg, a = 12.034(1) Å, is larger than all those reported previously (a = 11.981(6) Å, FENG et al. 1988; a = 12.001(2) Å, TSUKIMURA et al. 1993; a = 12.014(1) Å, KANAZAWA et al. 1997; a = 12.0173(1) Å, FUJITA et al. 2001). The larger unit-cell volume is probably due to the relatively high Fe contents in the sample.

The present results confirm that Fe-rich wadalite is isotypic with the other natural and synthetic members of the mayenite-group, $Ca_{12}Al_{14}O_{32}X$, where X is a partially occupied site hosting O^{2-}, S^{2-}, $2F^-$, $2OH^-$ or $2Cl^-$ (DUGDALE 1965, NURSE et al. 1965, WILLIAMS 1973, and references cited therein; CHRISTENSEN 1987, HOSONO & ABE 1987, FENG et al. 1988, IRVINE et al. 1988, SINGH & GLASSER 1988, GLASSER 1995, HAYASHI et al. 2002). In wadalite, ideally $Ca_{12}[(Al_{10}Si_4)O_{32}]Cl_6$, the X site is nearly fully occupied by Cl atoms. Thus, wadalite can be considered a Cl-enriched analogue of mayenite, $Ca_{12}Al_{14}O_{33}$, which is the mineral analogue of the well-known cement phase $C_{12}A_7$ and also a known high-temperature oxide ion-conductor, with charge-balance achieved by substituting Si for Al. Both wadalite and mayenite show a structural relation to the garnet group (e.g., FENG et al. 1988, TSUKIMURA et al. 1993, GLASSER 1995, STRUNZ & NICKEL 2001). Furthermore, it is noteworthy that the structure of wadalite can also be classified as one of the rare 3,4-connected, interrupted framework structures (LIEBAU 1985) with a $Q^3:Q^4$ value of 4 : 3. Additionally, an Al/Si disorder over both T-sites was already pointed out by FENG et al. (1988), which makes the applied generalised formula $M_{12}[(T2_8T1_6)O_{32}]X$ more appropriate.

Acknowledgements

The authors thank ALICE and EUGEN RONDORF, Neuwied, and GERHARD HENTSCHEL, Sinzig, for providing the rondorfite-, almarudite-, and wadalite-containing sample material, and HORST GEUER, Königswinter, for his useful comments. The financial support of the Österreichischer Akademischer Austauschdienst (under the Central European Exchange Program for University Students CCO–13/free mover), the Austrian Fonds zur Förderung der wissenschaftlichen Forschung FWF (Grants P15875–GEO

and P15220-GEO), and the International Centre for Diffraction Data (Grant 90-03) are gratefully acknowledged.

References

ARMBRUSTER, TH., BERMANEC, V., WENGER, M. & OBERHÄNSLI, R. (1989): Crystal chemistry of double-ring silicates: structure of natural and dehydrated milarite at 100K. – Eur. J. Miner. **1:** 353–362.

BAUR, W. H. & OHTA, T. (1982): The Si_5O_{16} pentamer in zunyite: refined and empirical relations for individual silicon–oxygen bonds. – Acta Crystallogr. B **38:** 390–401.

BRESE, N. E. & O'KEEFFE, M. (1991): Bond-valence parameters for solids. – Acta Crystallogr. B **47:** 192–197.

BROWN, I. D. (1996): *VALENCE*: a program for calculating bond valences. – J. Appl. Crystallogr. **29:** 479–480.

CHRISTENSEN, A. N. (1987): Neutron powder diffraction profile refinement studies on $Ca_{11.3}Al_{14}O_{32.3}$ and $CaClO(D_{0.88}H_{0.12})$. – Acta Chem. Scand. A **41:** 110–112.

DIRKEN, P. J., KENTGENS, A. P. M., NACHTEGAAL, G., VAN DER EERDEN, M. J. & JANSEN, J. B. H. (1995): Solid-state MAS NMR study of pentameric aluminosilicate groups with 180° intertetrahedral Al–O–Si angles in zunyite and harkerite. – Amer. Miner. **80:** 39–45.

DOWTY, E. (1999) ATOMS: A computer program for displaying atomic structures. – Kingsport TN 37663, U.S.A.

DUGDALE, R. A. (1965): $12CaO \cdot 7Al_2O_3$ phase in $CaO–Al_2O_3$ system. – Trans. Brit. Ceram. Soc. **64:** 324–332.

EFFENBERGER, H., GIESTER, G., KRAUSE, W. & BERNHARDT, H.-J. (1998): Tschörtnerite, a copper-bearing zeolite from the Bellberg volcano, Eifel, Germany. – Amer. Miner. **83:** 607–617.

FENG, Q. L., GLASSER, F. P., HOWIE, R. A. & LACHOWSKI, E. E. (1988): Chlorosilicate with the $12CaO \cdot 7Al_2O_3$ structure and its relationship to garnet. – Acta Crystallogr. C **44:** 589–592.

FISCHER, R. X. & TILLMANNS, E. (1988): The equivalent isotropic displacement factor. – Acta Crystallogr. C **44:** 775–776.

FISCHER, R. X., LENGAUER, C. L., TILLMANNS, E., ENSINK, R. J., REISS, C. A. & FANTNER, E. J. (1993): PC-Rietveld plus, a comprehensive Rietveld analysis package for PC. – Mater. Sci. Forum **133–136:** 287–292.

FRECHEN, J. (1971): Siebengebirge am Rhein, Laacher Vulkangebiet, Maargebirge der Westeifel. – Slg. Geol. Führer **56:** 209 pp. Gebr. Borntraeger (in German).

FUJITA, S., SUZUKI, K., OHKAWA, M., SHIBASAKI, Y. & MORI, T. (2001): Reaction of hydrogrossular with hydrogen chloride gas at high temperature. – Chem. Mater. **13:** 2523–2527.

GANDOLFI, G. (1964): Metodo per ottenere uno spettro di polveri da un cristallo singolo di piccole dimensioni (fino a 30 μ). – Miner. Petrogr. Acta **10:** 149–156 (in Italian).

GLASSER, F. P. (1995): Comments on wadalite, $Ca_6Al_5SiO_{16}Cl_3$, and the structures of garnet, mayenite and calcium chlorosilicate. Addendum. – Acta Crystallogr. C **51:** 340.

GIUSEPPETTI, G., MAZZI, F. & TADINI, C. (1977): The crystal structure of harkerite. – Amer. Miner. **62:** 263–272.

HAWTHORNE, F. C., KIMATA, M., ČERNÝ, P. & BALL, N. (1991): The crystal chemistry of the milarite-group minerals. – Amer. Miner. **76:** 1836–1856.

HAYASHI, K., HIRANO, M., MATSUISHI, S. & HOSONO, H. (2002): Microporous crystal $12CaO \cdot 7Al_2O_3$ encaging abundant O^- radicals. – J. Amer. Chem. Soc. **124:** 738–739.

HENTSCHEL, G. (1964): Mayenit, $12CaO \cdot 7Al_2O_3$, und Brownmillerit, $2CaO \cdot (Al, Fe)_2O_3$, zwei neue Minerale in den Kalksteineinschlüssen der Lava des Ettringer Bellerbergs. – N. Jb. Miner. Mh. **1964:** 22–29 (in German).

– (1987): Die Mineralien der Eifelvulkane. – 2nd extended Ed., Chr. Weise Verlag, Munich, Germany, 177 pp. (in German).

HOSONO, H. & ABE, Y. (1987): Occurrence of superoxide radical ion in crystalline calcium aluminate $12CaO \cdot 7Al_2O_3$ prepared via solid-state reactions. – Inorg. Chem. **26:** 1192–1195.

IRRAN, E., TILLMANNS, E. & HENTSCHEL, G. (1997): Ternesite, $Ca_5(SiO_4)_2(SO_4)$, a new mineral from the Ettringer Bellerberg/Eifel, Germany. – Miner. Petrol. **60:** 121–132.

IRVINE, J. T. S., LACERDA, M. & WEST, A. R. (1988): Oxide ion conductivity in $Ca_{12}Al_{14}O_{33}$. – Mater. Res. Bull. **23:** 1033–1038.

JASMUND, K. & HENTSCHEL, G. (1964): Seltene Mineralparagenesen in den Kalksteineinschlüssen der Lava des Ettringer Bellerbergs bei Mayen (Eifel). – Beitr. Miner. Petrogr. **10:** 296–314 (in German).

KAMB, W. B. (1960): Crystal structure of zunyite. – Acta Crystallogr. **13:** 15–23.

KANAZAWA, Y., AOKI, M. & TAKEDA, H. (1997): Wadalite, rustumite, and spurrite from La Negra mine, Queretaro, Mexico. – Chishitsu Chosasho Geppo **48:** 413–420.

KRAUSE, W., BLASS, G. & EFFENBERGER, H. (1999): Schäferite, a new vanadium garnet from the Bellberg volcano, Eifel, Germany. – N. Jb. Miner. Mh. **1999:** 123–134.

LENGAUER, C. L., TILLMANNS, E., NTAFLOS, TH. & HENTSCHEL, G. (1997): Neue Mineralfunde vom Bellerberg, Eifel. – Eur. J. Miner. **9** Bh. 1: 147 (in German).

LIEBAU, F. (1985): Structural chemistry of silicates. – Springer Verlag, Berlin, Heidelberg, Germany, 347 pp.

LIN, H., LIU, X. R. & PUN, E. Y. B. (2002): Sensitized luminescence and energy transfer in Ce^{3+} and Eu^{2+} codoped calcium magnesium chlorosilicate. – Opt. Mater. **18:** 397–401.

LOUISNATHAN, S. J. & GIBBS, G. V. (1972): Aluminium–silicon distribution in zunyite. – Amer. Miner. **57:** 1089–1108.

MACHIN, M. P. & MIEHE, G. (1976): Aluminum tetrasilicate $[Al(SiO_4)_4]^{13-}$ tetrahedral pentamers in harkerite. – N. Jb. Miner. Mh. **1976:** 228–232.

MANDARINO, J. A. (1981): The Gladstone-Dale relationship: Part IV. The compatibility concept and its application. – Canad. Miner. **19:** 441–450.

MIGHELL, A. D., HUBBARD, C. R. & STALICK, J. K. (1981): NBS*AIDS80: A FORTRAN program for crystallographic data evaluation. – NBS Technical Note 1141.

MIHAJLOVIĆ, T., LENGAUER, C. L., NTAFLOS, TH. & TILLMANNS, E. (2002): $^{[12]}K_2{}^{[6]}(Mn,Fe,Mg)_4{}^{[4]}(Be,Al)_6{}^{[4]}Si_{24}O_{60}$ – a new Mn-anlogue of milarite from the bellberg volcano, Eifel area, Germany. – 18th General Meeting IMA, Book of Abstracts A 12–13.

NURSE, R. W., WELCH, J. H. & MAJUMDAR, A. J. (1965): The $12CaO \cdot 7Al_2O_3$ phase in the $CaO–Al_2O_3$ system. – Trans. Brit. Ceram. Soc. **64:** 323–332.

OSTROVSKAYA, I. V. (1969): Crystal structures of sakhaite and harkerite. – Tr. Mineral. Muz. Akad. Nauk SSSR **19:** 197–201 (in Russian).

OTWINOWSKI, Z. & MINOR, W. (1997): Processing of X-ray diffraction data collected in oscillation mode. – In: CARTER, C. W. & SWEET, R. M. (eds.): Methods in Enzymology Series Vol. 276: Macromolecular Crystallography, part A, 307–326, Academic Press, San Diego.

PARK, N., JUNG, K. H., PARK, H. L., SONG, Y., MOON, H. S., KIM, K. C., MHO, S. I. & KIM, T. W. (1994): Photoluminescence and phase studies on $Ca_{8-x}Sr_xMg(SiO_4)_4Cl_2:Eu^{2+}$ phosphor. – J. Mater. Sci. Lett. **13:** 1252–1253.

PAULING, L. (1933): The crystal structure of zunyite $Al_{13}Si_5O_{20}(OH,F)_{18}Cl$. – Z. Kristallogr. **84:** 443–452.

SCHREYER, W., HENTSCHEL, G. & ABRAHAM, K. (1983): Osumilith in der Eifel und die Verwendung dieses Minerals als petrogenetischer Indikator. – Tschermaks Miner. Petrogr. Mitt. **31:** 215–234 (in German).

SCHÜLLER, W. (1990): Die Mineralien des Bellerberges bei Ettringen. – Lapis **15** (5): 9–35 (in German).

SHELDRICK, G. M. (1997): SHELXS–97 and SHELXL–97. – 2nd Version, Universität Göttingen, Göttingen, Germany.

SIEMENS INC. (1990): XPREP – reciprocal space exploration. – Version 4.2, Bruker AXS, Karlsruhe, Germany.

SINGH, V. K. & GLASSER, F. P. (1988): High-temperature reversible moisture uptake in calcium aluminate, $Ca_{12}Al_{14}O_{33-x}(OH)_{2x}$. – Ceram. Interntl. **14:** 59–62.

STRAUMANIS, M. & JEVINŠ, A. (1936): Präzisionsaufnahmen nach dem Verfahren von Debye und Scherrer. – II. Z. Physik **98:** 461–475.

STRUNZ, H. & NICKEL, E. H. (2001): Strunz Mineralogical Tables. – 9th Ed., Schweizerbart'sche Verlagsbuchhandlung, Stuttgart, Germany, 870 pp.

TSUKIMURA, K., KANAZAWA, Y., AOKI, M. & BUNNO, M. (1993): Structure of wadalite $Ca_6Al_5Si_2O_{16}C_{13}$. – Acta Crystallogr. C **49:** 205–207.

VON LAMPE, F., JOST, K. H., WALLIS, B. & LEIBNITZ, P. (1986): Synthesis, crystal structure and properties of a new calcium magnesium monosilicate chloride, $Ca_8Mg[(SiO_4)_4Cl_2]$. – Cem. Concr. Res. **16:** 624–632.

WILLIAMS, P. P. (1973): Refinement of the structure of $11CaO \cdot 7Al_2O_3 \cdot CaF_2$. – Acta Crystallogr. B **29:** 1550–1551.

WILSON, A. J. C. & PRINCE, E. (1999): International tables for crystallography, vol. C. Mathematical, physical and chemical tables. – 2nd Ed., Kluwer Academic Publishers, Dordrecht, The Netherlands, 992 pp.

YE, R. & WANG, X. (1985): Synthesis of a new compound $Ca_8Mg(SiO_4)_4Cl_2$. – Guisuanyan Xuebao **13:** 250–251 (in Chinese).

YE, R., WANG, X. & ZHANG, Z. (1987): Crystal structure of the new compound $Ca_8Mg(SiO_4)_4Cl_2$. – Guisuanyan Xuebao **15:** 309–314 (in Chinese).

ZHANG, X. & LIU, X. (1992): Luminescence properties and energy transfer of Eu^{2+} doped $Ca_8Mg(SiO_4)_4Cl_2$ phosphors. – J. Electrochem. Soc. **2:** 622–625.

Received: May 15, 2003; accepted: July 14, 2003

Author's addresses:

TAMARA MIHAJLOVIĆ, CHRISTIAN L. LENGAUER, UWE KOLITSCH, EKKEHART TILLMANNS, Institut für Mineralogie und Kristallographie, Universität Wien – Geozentrum, Althanstrasse 14, A-1090 Wien, Austria.

THEODOROS NTAFLOS, Institut für Geologische Wissenschaften, Universität Wien – Geozentrum, Althanstrasse 14, A-1090 Wien, Austria.

Corresponding author: CHRISTIAN L. LENGAUER, Fax: +431 4277 9532;
e-mail: christian.lengauer@univie.ac.at.